

# T2

*by* Pranowo Pranowo

---

**Submission date:** 07-Aug-2019 01:26PM (UTC+0700)

**Submission ID:** 1158288887

**File name:** ion\_of\_Seismic\_Wave\_Propagation\_Near\_a\_Fluid-Solid\_Interface.pdf (901.34K)

**Word count:** 3192

**Character count:** 16526

# NUMERICAL SIMULATION OF SEISMIC WAVE PROPAGATION NEAR A FLUID-SOLID INTERFACE

Pranowo<sup>1</sup>, Yoyok Adi Laksono<sup>2</sup>, Wiwit Suryanto<sup>3</sup>, Kirbani Brotopuspito<sup>3</sup>

<sup>1</sup> Department of Informatics Engineering, Atma Jaya Yogyakarta University (pran@staff.uajy.ac.id)

<sup>2</sup> PhD student of Department of Physics, Gadjah Mada University & Lecturer of Department of Physics, Malang State University

<sup>3</sup> Department of Physics, Gadjah Mada University

## ABSTRACT

We introduce a high-order discontinuous galerkin method for modeling wave propagation in complex media with both fluid (acoustic) and solid (elastic) medium, as for instance in offshore seismic experiments. The problem is formulated in terms of velocity-stress in both media. A nodal high order discontinuous galerkin finite element is used for the spatial discretization while an explicit low storage fourth order Runge Kutta scheme is used to march in the time domain. The numerical scheme provides stable and accurate methods for simulating seismic wave across a fluid – solid interface, the comparisons with finite element method and analytical solutions show a good agreement.

**Keywords:** seismic wave, fluid – solid interface, discontinuous galerkin.

## 1. INTRODUCTION

Seismic wave propagation near fluid-solid interface problems are found in many scientific and engineering applications such as:

- Seismic exploration in marine environment
- Interaction seismic wave with reservoir dam
- Earthquake induced tsunami

Until now, these problems are still open research area. Many researchers has investigated these problems experimentally or numerically. Physical modeling has been successfully used in investigation of the seismic wave along liquid-solid interfaces (Person, 1999), from her experimental results she can identify the modes of propagation of interfaces waves, measure velocities, attenuation and re-radiation of these waves. The drawbacks of experimental approach are the measurement and data processing are so complicated, the measurement accuracy depended on the operator skill and the physical models are not easy to be built and expensive. Supporting by tremendous of the increase computational power, numerical modeling has become an important research area. Much attention has been paid by many researchers to solve the seismic wave propagation near fluid-solid interface problems by using numerical approach. Assuming solid as elastic

medium and fluid as acoustic medium is sufficient in that context. Based on that assumption the wave propagation in solid medium can be modeled by elastodynamic equations and the wave propagation in fluid medium can be modeled by acoustic equations. One needs to model wave propagation in fluid as well in the underlying solid.

The oldest and the famous numerical method that have been used widely to model seismic wave propagation in time domain is finite difference method (FDM). Van Vossen et al. (2002) used this method to model seismic wave propagation in fluid-solid configuration. The wave motion is governed by equation of motion and the elastic constitutive equation which are written in a first-order hyperbolic equation system for unknown components of stress and particle velocity. In the fluid medium the Lamé's coefficients  $\mu$  is set to be equal zero. A dipping interface is represented by staircase of vertical and horizontal fluid-solid boundary segments in the numerical scheme and properties of medium near the interface are calculated using arithmetic average. Van Vossen et al. (2002) showed that the accuracy of the FDM is good for small dipping but poor for large dipping angle ( $> 30^\circ$ ). This is the main drawback of FDM which can not be used for modeling of irregular domain.

Diaz and Joly (2005) proposed nonconforming finite element method for solving time dependent fluid-structure interaction problems. They used different formulations for both fluid and solid media. Pressure-velocity formulation is used in fluid medium and velocity-stress formulation is used in solid medium. The coupling between the fluid and solid is done via continuity of normal velocities and of normal stresses. They used staggered mesh for both spatial and temporal domain as FDM did for minimizing the dispersion error. They showed that their numerical results have good agreement with analytical solutions. The use of staggered mesh made the numerical algorithm more complicated and the application of the method is limited for simple spatial domain only.

Komatitsch et al. (2000, 2011) and Madec et al. (2009) developed a high order spectral element method (SEM) for simulating seismic wave propagation near a fluid-solid interface. They showed that SEM is an efficient tool for modeling wave propagation in complex structures, and high order accuracy can be achieved. The spectral element method is developed from conventional finite element method by replacing the basis function with the higher order legendre polynomials. They used second order hyperbolic equation system i.e. velocity potential formulation for fluid medium and displacement formulation for solid medium. The semi discrete equations are integrated in time using explicit predictor-corrector staggered time scheme. This time integration has only second order accuracy.

Wilcox et al. (2010) developed a high order discontinuous galerkin method (DGM) for modeling seismic wave through coupled three dimensional elastic-acoustic media. They used first-order hyperbolic equation system for unknown components of strain and particle velocity. In the fluid medium the Lamé's coefficients  $\mu$  is set to be equal zero. The DG methods allow unstructured mesh configuration and inter-element continuity is not required. The basis function is discontinuous across mesh boundaries. Through a proper choices of flux computation points, the method only requires communication between mesh that have common faces. No global matrix inversion is required and the problem can be solved locally in each mesh. In

their approach, they divided the spatial domain into hexahedral elements. Higher order accuracy can be achieved easily by increasing the order of basis function polynomials.

In this paper we develop a high order discontinuous galerkin (DG) method for simulating two dimensional seismic wave near fluid-solid interface. The wave motion in both fluid and solid media is governed by elastodynamics equations in the form of velocity-stress formulation. The spatial domain is divided into unstructured triangular elements. Perfectly matched layer (PML) is used as as absorbing boundary condition.

## 2. GOVERNING EQUATIONS

Our approach of treating seismic waves numerically is based on the theory elastodynamics. We use the velocity-stress formulation as the governing equations:

$$\begin{aligned} \frac{\partial v_x}{\partial t} - \frac{1}{\rho} \left( \frac{\partial \tau_{xx}}{\partial x} + \frac{\partial \tau_{xy}}{\partial y} \right) &= f_x & ; & & \frac{\partial v_y}{\partial t} - \frac{1}{\rho} \left( \frac{\partial \tau_{xy}}{\partial x} + \frac{\partial \tau_{yy}}{\partial y} \right) &= f_y \\ \frac{\partial \tau_{xx}}{\partial t} - (\lambda + 2\mu) \frac{\partial v_x}{\partial x} - \lambda \frac{\partial v_y}{\partial y} &= 0 & ; & & \frac{\partial \tau_{yy}}{\partial t} - \lambda \frac{\partial v_x}{\partial x} - (\lambda + 2\mu) \frac{\partial v_y}{\partial y} &= 0 \\ \frac{\partial \tau_{xy}}{\partial t} - \mu \left( \frac{\partial v_x}{\partial y} + \frac{\partial v_y}{\partial x} \right) &= 0 \end{aligned} \quad (1)$$

In which  $v_x$  and  $v_y$  are the components of velocity vectors,  $\tau_{xx}$ ,  $\tau_{yy}$  dan  $\tau_{xy}$  are the elements of the stress tensor and  $(f_x, f_y)$  are body force vector. The elastic medium is described by the density and the Lamé coefficients  $\lambda(x, y)$  &  $\mu(x, y)$ . In the fluid medium the Lamé coefficients  $\mu(x, y)$  is set to be zero

## 3. PERFECTLY MATCHED LAYER

The simulation of seismic waves by discontinuous galerkin method in unbounded domains requires a specific boundary condition of the necessarily truncated computational domain. We propose an absorbing boundary condition called perfectly matched layer (PML). Presented in time domain electromagnetic simulations (Berenger, 1996), PML has since been used extensively in that field. PML has also been incorporated into a variety of wave propagation algorithms. Colino and Tsogka (2001) have formulated and demonstrated PML in the P-SV case via Virieux (1986) finite difference scheme and a mixed finite element algorithms. Excellent results were demonstrated in homogeneous and heterogeneous media, including anisotropy in the finite element scheme.

Starting with the system of equations (1), each equation is split into a parallel and perpendicular component, based on spatial derivative separation. That is, the perpendicular equations contains the spatial derivative term which acts normal to the coordinate plane of interest and a damping term, and the parallel equation

contain the remaining spatial derivative terms. Finally, an additional equation is required to sum the results of the split equations

$$\begin{aligned}
 \frac{\partial v_{xx}}{\partial t} + \sigma(x)v_{xx} &= \frac{1}{\rho} \frac{\partial \tau_{xx}}{\partial x} + f_x & ; & \quad \frac{\partial v_{yy}}{\partial t} + \sigma(y)v_{yy} = \frac{1}{\rho} \frac{\partial \tau_{yy}}{\partial y} \\
 \frac{\partial v_{yx}}{\partial t} + \sigma(x)v_{yx} &= \frac{1}{\rho} \frac{\partial \tau_{xy}}{\partial x} & ; & \quad \frac{\partial v_{xy}}{\partial t} + \sigma(y)v_{xy} = \frac{1}{\rho} \frac{\partial \tau_{yx}}{\partial y} + f_y \\
 \frac{\partial \tau_{xxx}}{\partial t} + \sigma(x)\tau_{xxx} &= (\lambda + 2\mu) \frac{\partial v_x}{\partial x} & ; & \quad \frac{\partial \tau_{xyy}}{\partial t} + \sigma(y)\tau_{xyy} = \lambda \frac{\partial v_y}{\partial y} \\
 \frac{\partial \tau_{yyx}}{\partial t} + \sigma(x)\tau_{yyx} &= \lambda \frac{\partial v_x}{\partial x} & ; & \quad \frac{\partial \tau_{yyy}}{\partial t} + \sigma(y)\tau_{yyy} = (\lambda + 2\mu) \frac{\partial v_y}{\partial y} \\
 \frac{\partial \tau_{xyx}}{\partial t} + \sigma(x)v_{xyx} &= \mu \frac{\partial v_y}{\partial x} & ; & \quad \frac{\partial \tau_{xyy}}{\partial t} + \sigma(y)v_{xyy} = \mu \frac{\partial v_x}{\partial y}
 \end{aligned} \tag{2}$$

$$v_x = v_{xx} + v_{xy}, \quad v_y = v_{yx} + v_{yy}, \quad \tau_{xx} = \tau_{xxx} + \tau_{xyx}, \quad \tau_{yy} = \tau_{yyx} + \tau_{yyy}, \quad \tau_{xy} = \tau_{xyx} + \tau_{xyy}$$

**7** In the absorbing layers we use the following model for the damping parameters:

$$\sigma(x) = d_0 \left( \frac{x}{\delta} \right)^2; \quad \sigma(y) = d_0 \left( \frac{y}{\delta} \right)^2 \quad \text{and} \quad d_0 = \log \left( \frac{1}{R} \right) \frac{3c_p}{2\lambda}$$

where  $\delta$  is the length of the layer and  $d_0$  is a function of the theoretical reflection coefficient ( $R$ )

For simplicity, the split equations (2) are written in vector form as follows:

$$\frac{\partial \mathbf{q}}{\partial t} + \mathbf{A} \frac{\partial \mathbf{q}}{\partial x} + \mathbf{B} \frac{\partial \mathbf{q}}{\partial y} = \mathbf{f} \tag{3}$$

where  $\mathbf{q} = [v_{xx} \quad v_{yy} \quad v_{yx} \quad v_{xy} \quad \tau_{xxx} \quad \tau_{xyx} \quad \tau_{yyx} \quad \tau_{yyy} \quad \tau_{xyx} \quad \tau_{xyy}]^T$

#### 4. DISCONTINUOUS GALERKIN METHOD

**3** The spatial derivatives are discretized by using a discontinuous galerkin method. The simplified of Eq.(1) according to Galerkin's procedure using the same basis function  $\phi$  within each element is defined below (Hesthaven & Warburton, 2002; 2008)

$$\begin{aligned} \left( \phi, \frac{\partial \mathbf{q}}{\partial t} + \mathbf{A} \frac{\partial \mathbf{q}}{\partial x} + \mathbf{B} \frac{\partial \mathbf{q}}{\partial y} \right) &= 0 \\ \Leftrightarrow \left( \phi, \frac{\partial \mathbf{q}}{\partial t} \right)_{\Omega} + \left( \phi, \mathbf{A} n_x \mathbf{q} + \mathbf{B} n_y \mathbf{q} \right)_{\partial \Omega} - \left( \frac{\partial}{\partial x} (\mathbf{A} \phi), \mathbf{q} \right)_{\partial \Omega} - \left( \frac{\partial}{\partial y} (\mathbf{B} \phi), \mathbf{q} \right)_{\partial \Omega} &= 0 \end{aligned} \quad (4)$$

Here  $(\cdot, \cdot)$  represents the normal  $2L$  inner product, the second term is flux vector and  $(n_x, n_y)$  are normal vector. The mathematical manipulation of the flux vector is calculated as below:

$$\left( \phi, \frac{\partial \mathbf{q}}{\partial t} + \mathbf{A} \frac{\partial \mathbf{q}}{\partial x} + \mathbf{B} \frac{\partial \mathbf{q}}{\partial y} \right)_{\Omega} + \left( \phi, \mathbf{A} n_x + \mathbf{B} n_y \right) (\hat{\mathbf{q}} - \mathbf{q}^-)_{\partial \Omega} = 0 \quad (5)$$

where  $\mathbf{q}^-|_{\partial \Omega} = \hat{\mathbf{q}}^-(\mathbf{q}^-, \mathbf{q}^+)|_{\partial \Omega}$  and the last term of equation (3) is called numerical flux.

The numerical flux along three sides of triangular element is calculated by Lax Friedrich flux.

$$\left( \phi, \mathbf{A} n_x + \mathbf{B} n_y \right) (\hat{\mathbf{q}} - \mathbf{q}^-)_{\partial \Omega} = \left( \phi, \mathbf{A} n_x + \mathbf{B} n_y + C_p \right) (\mathbf{q}^+ - \mathbf{q}^-) / 2 \quad (6)$$

Here, we took the Kornwinder Dubiner function on straight sided triangle as the basis written in equation 7 (see Figs. 1 and 2):

$$\phi_j(r, s) = \sqrt{\frac{2i+1}{2}} \sqrt{\frac{2i+2j+2}{2}} P_i^{0,0} \left( \frac{2(1+r)}{(1-s)} - 1 \right) P_j^{2=+1,0}(s) \quad (7)$$

where,  $P^{\alpha,\beta}$  is orthogonal Jacobi polynomial

All straight sided triangles are the image of this triangle under the map:

$$\begin{pmatrix} x \\ y \end{pmatrix} = -\left( \frac{r+s}{2} \right) \begin{pmatrix} v_x^1 \\ v_y^1 \end{pmatrix} + \left( \frac{1+r}{2} \right) \begin{pmatrix} v_x^2 \\ v_y^2 \end{pmatrix} + \left( \frac{1+s}{2} \right) \begin{pmatrix} v_x^3 \\ v_y^3 \end{pmatrix} \quad (8)$$

The set of points in the triangle, which we can build the Lagrange interpolating polynomials, can be viewed as Gauss-Legendre–Lobatto (GLL) points.

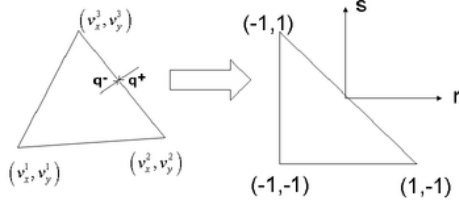


**Figure 1: Coordinate Transformation**

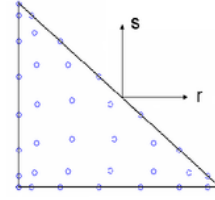


**Figure 2: Seventh Order Gauss Lobatto Quadrature Nodes**

The vector  $\mathbf{q}$  is expanded using equation (3), we take expansion of  $v_x$  as example:

$$v_x(r, s) = \sum_{i=0}^N \sum_{j=0}^{N-i} \phi_{ij}(r, s) \hat{v}_{xij} \quad (9)$$

$$v_x(r_n, s_n) = \sum_{m=1}^{m=M} \mathbf{V}_{nm} \hat{v}_{xm} \quad (10)$$

$$\hat{v}_{xm} = \sum_{m=1}^{m=M} (\mathbf{V}^{-1})_{mj} v_x(r_j, s_j)$$

$$\begin{aligned} \frac{\partial v_x}{\partial r}(r, s) &= \sum_{i=0}^N \sum_{j=0}^{N-i} \frac{\partial \phi_{ij}}{\partial r}(r, s) \hat{v}_{xij} = \hat{\mathbf{D}}^r \mathbf{V}^{-1} v_x(r, s) & \hat{\mathbf{D}}^r &= \frac{\partial \phi}{\partial r} \\ \frac{\partial v_x}{\partial s}(r, s) &= \sum_{i=0}^N \sum_{j=0}^{N-i} \frac{\partial \phi_{ij}}{\partial s}(r, s) \hat{v}_{xij} = \hat{\mathbf{D}}^s \mathbf{V}^{-1} v_x(r, s) & \hat{\mathbf{D}}^s &= \frac{\partial \phi}{\partial s} \end{aligned}$$

where  $\mathbf{V}_{ij}$  and  $N$  are Vandermonde matrix and the order of Jacobi polynomial respectively.

The semi discrete Eq. (4) is integrated in time marching by using five stage of fourth order 2N-storage Runge-Kutta scheme as developed by Carpenter & Kennedy (1994). The final equations are found as written in Eq. (11).

$$\frac{d\mathbf{q}}{dt} = L[t, \mathbf{q}(t)] \quad (11)$$

$$d\mathbf{q}_j = A_j d\mathbf{q}_{j-1} + dt L(\mathbf{q}_j)$$

$$\mathbf{q}_j = \mathbf{q}_{j-1} + B_j + d\mathbf{q}_j$$

where  $dt$  is the time step. The vectors  $A$  and  $B$  are the coefficients that will be used to determine the properties of the scheme. The maximum time step is (Hesthaven and Warburton, 2002):

$$\Delta t \leq \frac{2h}{c_p(N-1)^2} \quad (12)$$

where  $c_p$  is primary wave velocity and  $h$  is the smallest edge length of the element

## 5. RESULTS AND DISCUSSION

In this section we present two numerical examples. The first example aims at showing the accuracy of DGM compared to analytical solution and Fem which proposed by Diaz et al. (2004) and the second example aims at showing that DGM can easily handle problems with complicated interface.

### 5.1. Numerical Example I

The first example has a simple configuration: two half-planes separated by a straight interface, one constitutes the fluid medium and the second one constitutes solid medium. The material properties for the fluid are  $c_p = 1500 \text{ ms}^{-1}$ ,  $c_s = 0 \text{ ms}^{-1}$  and  $\rho = 1000 \text{ kg m}^{-3}$  and the material properties for the solid are  $c_p = 4000 \text{ ms}^{-1}$ ,  $c_s = 1800 \text{ ms}^{-1}$  and  $\rho = 1850 \text{ kg m}^{-3}$ . The size of each medium is  $20 \text{ mm} \times 5 \text{ mm}$ . We added absorbing layer surrounding the domain with the thickness of the layer equals  $1 \text{ mm}$  and total number of triangular elements is 15060. The polynomial degree is  $N = 3$  and the time step  $\Delta t = 10^{-8} \text{ s}$ . The source function is a point source located in the fluid at  $2 \text{ mm}$  above the interface, the time variation of the source is given as Gaussian with dominating frequency is  $1 \text{ MHz}$ .

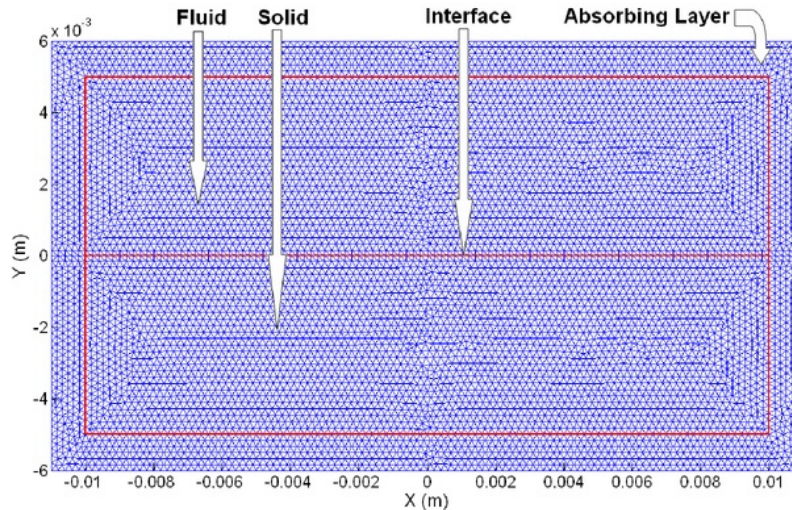


**Figure 3: Mesh of first example**

Snapshots of the first example can be seen in figure 4a – 4f.



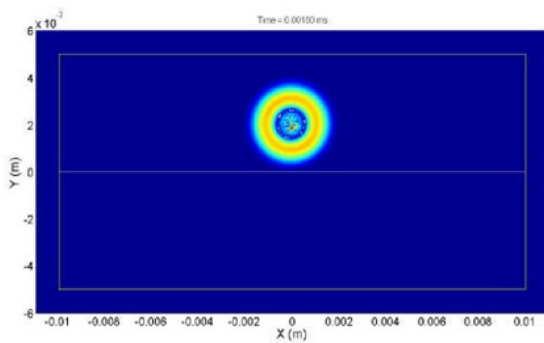


**Figure 4a: Velocity fields of 1<sup>st</sup> example at 0.18  $\mu$ s**

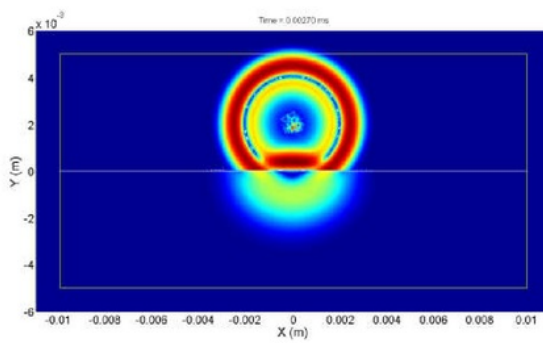


**Figure 4b: Velocity fields of 1<sup>st</sup> example at 0.27  $\mu$ s**

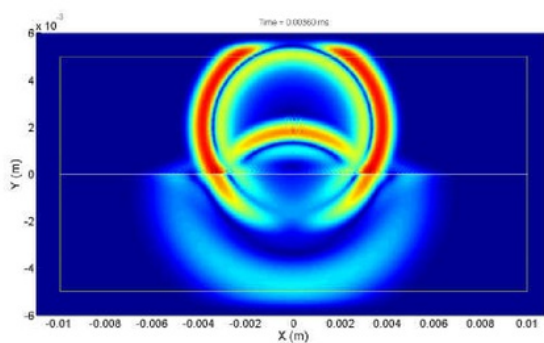


**Figure 4c: Velocity fields of 1<sup>st</sup> example at 0.36  $\mu$ s**

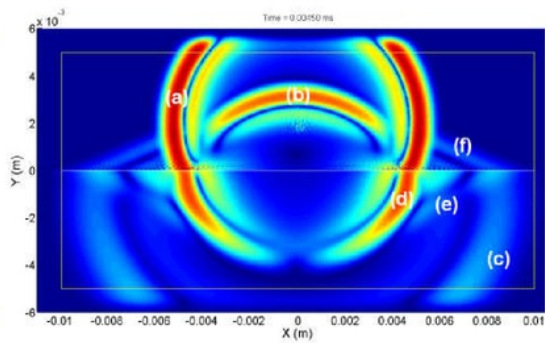


**Figure 4d: Velocity fields of 1<sup>st</sup> example at 0.45  $\mu$ s**

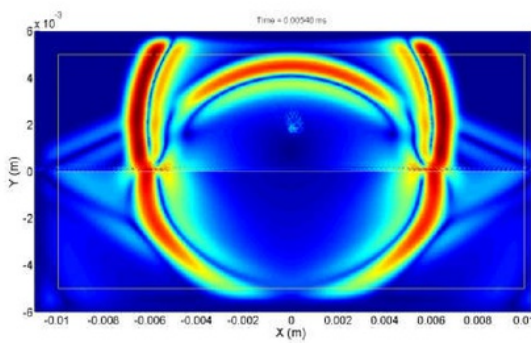


**Figure 4e: Velocity fields of 1<sup>st</sup> example at 0.54  $\mu$ s**

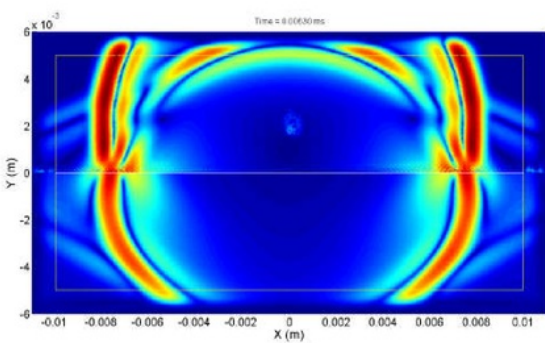


**Figure 4f: Velocity fields of 1<sup>st</sup> example at 0.63  $\mu$ s**

Figure (4d) shows that the direct wave (a) and reflected wave can be observed in the fluid, the transmitted P (c) and P-to-S converted (d) waves are clearly visible in the solid. Significant refracted waves are also present (e, f, g).

To validate the DG method, we compare the numerical DGM (the green curve) solution to the FEM solution (the red curve) and analytical solution (the blue curve) which are provided by Diaz et al. (2005). The two components of the numerical and analytical velocity are shown by figure 5a and 5b. The curves are perfectly superimposed, showing the good accuracy of DGM.

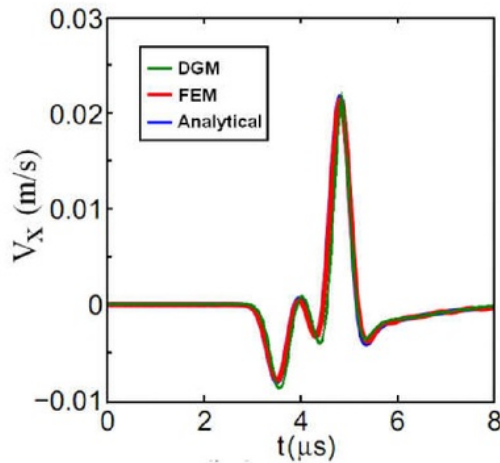


Figure 5a: Horizontal velocity ( $v_x$ )

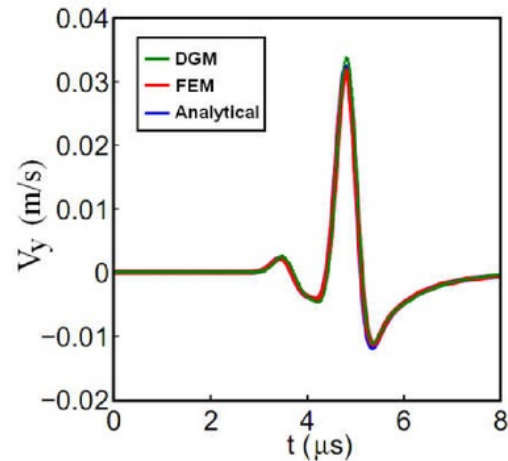


Figure 5b: Vertical velocity ( $v_y$ )

From 4a – 4f we can see no reflection on the left, right and bottom edges. The PML absorbed the outgoing waves well.

## 5.2. Numerical Example II

This example is taken from Komatitsch et al. (2000). The domain of the second example consists of two homogeneous half-spaces in contact at a sinusoidal interface, as shown in figure 6. The lower part of the model is elastic, while the upper part is acoustic, a water layer. The material properties for the water are  $c_p = 1500 \text{ ms}^{-1}$ ,  $c_s = 0 \text{ ms}^{-1}$  and  $\rho = 1020 \text{ kg m}^{-3}$  and the material properties for the solid are  $c_p = 3400 \text{ ms}^{-1}$ ,  $c_s = 1963 \text{ ms}^{-1}$  and  $\rho = 2500 \text{ kg m}^{-3}$ . Total number of triangular elements is 13876.

The polynomial degree is  $N = 5$  and the time step  $\Delta t = 10^{-2} \text{ s}$ . The source function is a point source located in the fluid at  $x = 2900 \text{ m}$  and  $y = 3098 \text{ m}$ , the time variation of the source is given as Ricker (i.e., the first derivative of a Gaussian) with dominating frequency is 7 Hz.

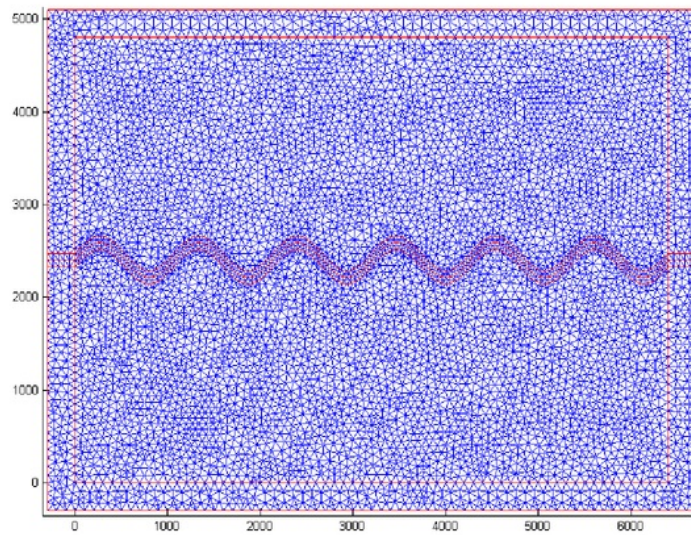


Figure 6: Mesh of second example

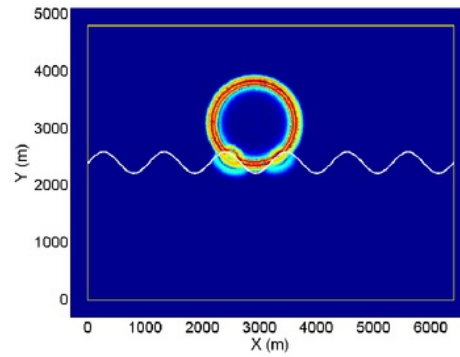
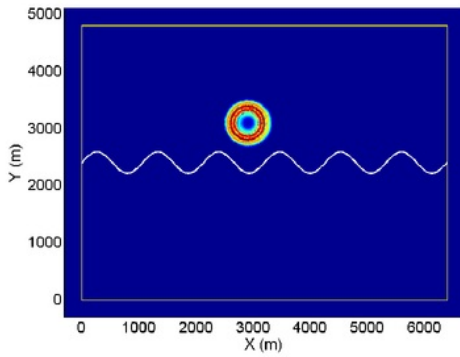


Figure 7a: Velocity fields of 2<sup>nd</sup> example at 0.3 s

Figure 7b: Velocity fields of 2<sup>nd</sup> example at 0.6 s

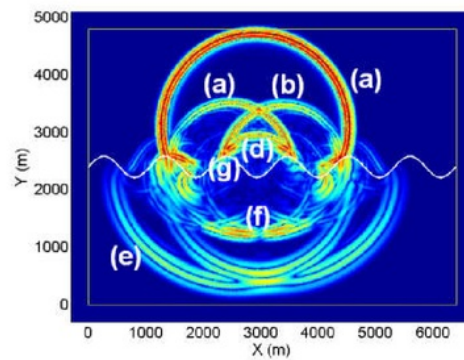
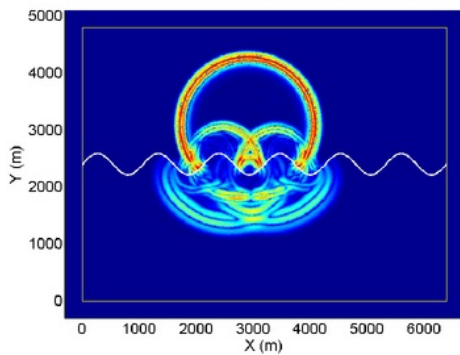


Figure 7c: Velocity fields of 2<sup>nd</sup> example at 0.9 s

Figure 7d: Velocity fields of 2<sup>nd</sup> example at 1.2 s

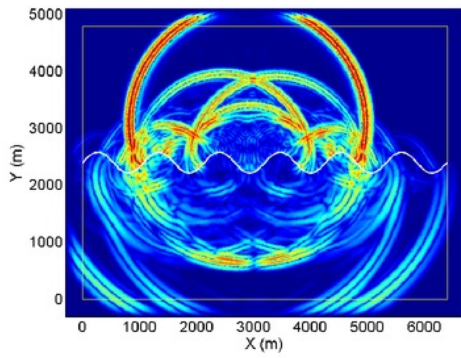


Figure 7e: Velocity fields of 2<sup>nd</sup> example at 1.5 s

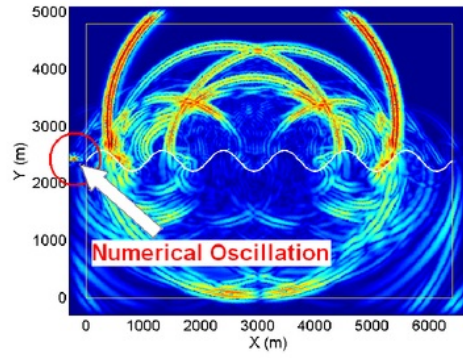


Figure 7f: Velocity fields of 2<sup>nd</sup> example at 1.8s

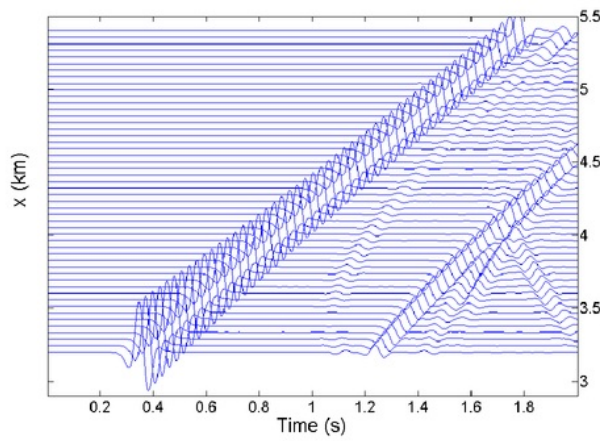


Figure 8a: Seismogram of  $(v_x)$  of DGM

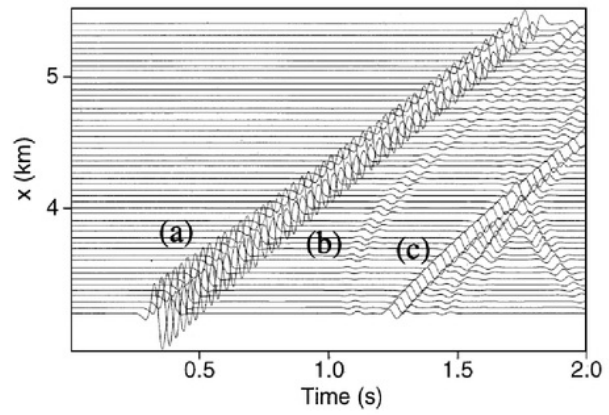


Figure 8b: Seismogram of  $(v_x)$  of SEM

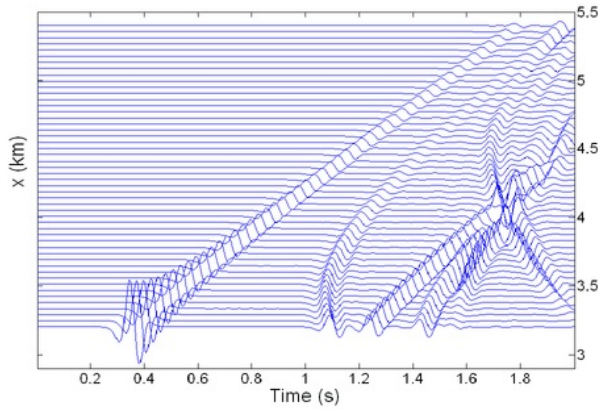


Figure 9a: Seismogram of  $(v_y)$  of DGM

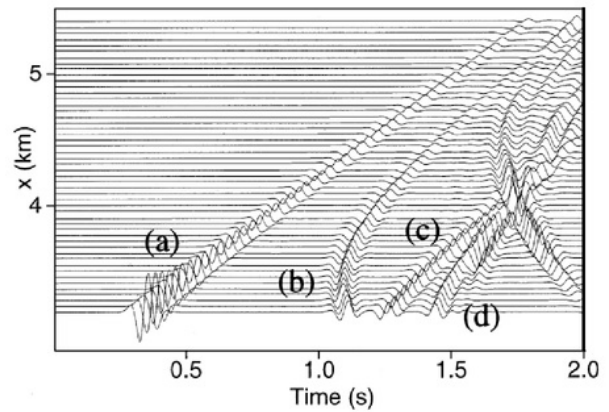


Figure 9b: Seismogram of  $(v_y)$  of SEM

Figure 6a – 6f show the snapshots of seismic wave propagation in two-layered media at  $t = 0.3$ ,  $t = 0.6$ ,  $t = 0.9$ ,  $t = 1.2$ ,  $t = 1.5$ , and  $t = 1.8$  s. Mode conversions of wave reflected at the interface are clearly visible. The entire wavefields are composed of various waves as described by Komatitsch et al. (2000), i.e. (a) the direct P-wave, (b) the strongly curved reflected P-wave on the first anticline on the right, (c) the P-wave reflected off the first anticline on the left [symmetric of phase (b)], (d) the P-wave reflected off the central syncline, which undergoes a time delay and therefore a triplication, (e) various transmitted P-waves, (f) various transmitted P-to-S converted waves, and (h) a slow phase traveling along the interface, which is interpreted to be a Stoneley wave.

Comparisons of seismograms between DGM and SEM results are shown in figure 8a- 8b and 9a -9b. Those figures show a good agreement. Although the numerical calculations show an excellent results, the modeling of fluid medium by using velocity-stress formulation has a drawback. This formulation will generate a small parasitic S-waves near the interface. This parasitic S-waves will be accumulated for long time simulation and can destroy the stability of the numerical scheme.

## 9 6. CONCLUSIONS AND FUTURE WORKS

We have introduced that the use of high-order discontinuous galerkin methods allows one to model seismic wave propagation across a fluid – solid interface. The numerical scheme provides stable and accurate methods for simulating seismic wave, the comparisons with finite element method and analytical solutions show a good agreement.

Numerical results have shown that the use of velocity-stress formulation will generate very small parasitic S-waves near the interfaces. Therefore in the future we will use velocity strain formulation instead velocity-stress formulation for modeling seismic wave near fluid-solid interface.

## REFERENCES

- Berenger, J. P. (1996). Three-Dimensional Perfectly Matched Layer for the Absorption of Electromagnetic Waves. *Journal Computational Physics*, 127, pp. 1363-379.
- Carpenter, M. H.; and Kennedy, C. A. (1994). Fourth-order 2N-Storage Runge-Kutta Schemes. NASA Technical Memorandum 109112, NASA Langley Research Center, Hampton, Virginia.
- Collino, F.; and Tsogka, C. (2001), Application of the PML absorbing layer model to the linear elastodynamic problem in anisotropic heterogeneous medium. *Geophysical Journal International*, Vol. 66, No. 1, pp. 294-307, 2001
- Diaz, J.; and Patrick, J. (2005). Robust high order non-conforming finite element formulation for time domain fluid-structure interaction. *Journal of Computational Acoustics*, World Scientific, 13 (3), pp. 403-431.

- Hesthaven, J. S.; and Warburton, T. (2002). High-order Nodal Methods on Unstructured Grids, I. Time Domain Solution of Maxwell's Equation. *J. Computational Physics*, 181, pp. 1-34.
- Hesthaven, J. S.; and Warburton, T. (2008). *Nodal Discontinuous Galerkin Methods: Algorithms, Analysis, and Applications*, Springer, New York.
- Komatitsch, D.; Barnes, C.; Tromp, J. (2000). Wave propagation near a fluid-solid interface: a spectral element approach. *Geophysics*, vol. 65, p. 623-631.
- Komatitsch, D. (2011). Fluid-solid coupling on a cluster of GPU graphics cards for seismic wave propagation. *Comptes Rendus de l'Académie des Sciences – Mécanique*, vol. 339, p. 125-135
- Madec, R.; Komatitsch, D.; and Diaz, J. (2009). Energy-conserving local time stepping based on high-order finite elements for seismic wave propagation across a fluid-solid interface. *Computer Modeling in Engineering and Sciences*, vol. 49(2), p. 163-189.
- Person, E. (1999). Experimentally study of wave propagation along a liquid-solid interface. Report No.: GPM 2/99, Department of Exploration Geophysics, Curtin University of Technology, Australia.
- Van Vossen, R.; Robertsson, J.O.A.; and Chapman, C.H. (2002). Finite-difference modeling of wave propagation in a fluid-solid configuration. *Geophysics*, vol. 67, p. 618-624.
- Wilcox, L.C. et al. (2010). A high-order discontinuous Galerkin method for wave propagation through coupled elastic-acoustic media. *Journal of Computational Physics*, **229**, Nr. 24, pp. 9373-9396

## ORIGINALITY REPORT

---

<b>25%</b>	<b>17%</b>	<b>18%</b>	<b>2%</b>
SIMILARITY INDEX	INTERNET SOURCES	PUBLICATIONS	STUDENT PAPERS

---

## PRIMARY SOURCES

---

<b>1</b>	<b>web.univ-pau.fr</b> Internet Source	<b>6%</b>
<b>2</b>	Carey Marcinkovich. "On the implementation of perfectly matched layers in a three-dimensional fourth-order velocity-stress finite difference scheme", Journal of Geophysical Research, 2003 Publication	<b>4%</b>
<b>3</b>	<b>www.scribd.com</b> Internet Source	<b>3%</b>
<b>4</b>	Pranowo Pranowo, Djoko Budiyanto Setyohadi. "Numerical simulation of electromagnetic radiation using high-order discontinuous galerkin time domain method", International Journal of Electrical and Computer Engineering (IJECE), 2019 Publication	<b>2%</b>
<b>5</b>	<b>quakes.uq.edu.au</b> Internet Source	<b>2%</b>

---

6

Internet Source

2%

7

Joly, P, and C Tsogka. "Numerical Methods for Treating Unbounded Media", Numerical Insights, 2008.

Publication

1%

8

Yao-Chong Sun, Wei Zhang, Jian-Kuan Xu, Xiaofei Chen. "Numerical simulation of 2-D seismic wave propagation in the presence of a topographic fluid–solid interface at the sea bottom by the curvilinear grid finite-difference method", Geophysical Journal International, 2017

Publication

1%

9

Lecture Notes in Computer Science, 2012.

Publication

1%

10

Xiomara Contreras. "Wave propagation in a 3D fluid-solid configuration: Staggered-grid finite-difference modeling and stability analysis", SEG Technical Program Expanded Abstracts, 2011

Publication

1%

11

[hal.inria.fr](http://hal.inria.fr)

Internet Source

1%

12

[academic.oup.com](http://academic.oup.com)

Internet Source

1%

LUCA, Adrian, Regis Marchiano, and Jean-



13

Camille CHASSAING. "Numerical Simulation of Transit-Time Ultrasonic Flowmeters by a Direct Approach", IEEE Transactions on Ultrasonics Ferroelectrics and Frequency Control, 2016.

1%

Publication

---

Exclude quotes On

Exclude matches < 1%

Exclude bibliography On

T2

---

GRADEMARK REPORT

---

FINAL GRADE

/0

GENERAL COMMENTS

**Instructor**

---

PAGE 1

---

PAGE 2

---

PAGE 3

---

PAGE 4

---

PAGE 5

---

PAGE 6

---

PAGE 7

---

PAGE 8

---

PAGE 9

---

PAGE 10

---

PAGE 11

---

PAGE 12

---

PAGE 13

---